

Innovative Application of FRPs for Seismic Strengthening of RC Shear Wall

by K. Kobayashi

Synopsis: The small holes were drilled at the grid intersection on the concrete wall panel. A bundle of aramid strands was passed through the holes so that it sewed them in cross diagonal directions. As a result, the concrete wall panel was shut up into a net made of aramid sewing bands. Shear capacity increased by more than 25%. FRP sewing bands worked as confinement to the concrete under compressive stress rather than the tensile braces. Its performance is expected to be better than that reinforced by FRP sheet wrapping system, and more strengthening effect will be obtained with less amount of fiber material. This strengthening idea is originally proposed to apply it to the infill-brick wall. The concept and the effectiveness of the idea were verified by the tests on the scaled RC shear wall.

Keywords: aramid fiber; FRP; seismic strengthening; shear wall

1270 Kobayashi

Katsumi Kobayashi studied architecture and building engineering at Tokyo Institute of Technology (TIT) and was given the degree of Dr. of Engineering in 1981. He worked at RLEM, TIT during 1981-1987 and initiated a research for FRPs. He moved to University of Fukui in 1987 and a full professor since 1993.

INTRODUCTION

In Kocaeli earthquake^[1] in 1999, the infill-bricks collapsed out of the frame as shown in Fig.1 and a large number of buildings were totally collapsed as shown in Fig.2 because of the poor detail of beam-column connections. This infill-brick wall is non-structural element. The primary objective of this proposed method is to expect the infill-brick wall to carry the horizontal force by keeping the bricks inside the frame and fixing them to the beams and columns. This type of structure is popular in many seismic countries, and it is required to be strengthened with less expensive cost.

As the first phase, the effectiveness of the proposed method will be verified and evaluated by applying it to RC shear wall panel. The bands made of continuous fiber materials are installed crossing the cracks on the wall panel. They resist to the expansion of cracks, and transfer the tensile force over the cracks. Bayrak and Binici^[2] made a similar application of FRP bands to the flat slab system to increase the punching shear capacity, and obtained a satisfied result. This proposed method is on the extension of the idea of Bayrak and Binici^[2]

The strengthening method of RC shear wall using carbon fiber (CF) sheet has been already developed^[4]. CF sheet is bonded on the overall surface of the wall panel. However, once the cracks occur, CF sheet delaminates easily and the shear capacity gain is restricted comparatively with the fairly large amount of CF sheet. The biggest advantage of the proposed method is to be able to secure the enough anchoring strength of the fiber materials on the wall. In the construction procedure, there are many advantages as described below. The installation technique is somewhat complicated, but it is not a difficult technique. The quality control will be easier than the conventional method^[4]. Furthermore it has a potential to reduce the use of the amount of the materials.

This project is now ongoing supported by Grant-in-Aid for Scientific Research of JSPS. This paper will describe the results of the pilot test and the beginning result of the phase-1 test program.

RESEARCH SIGNIFICANCE

The original target of the proposed method is the vulnerable building with infill-brick wall that collapsed into the shape of pancake during the past earthquakes and brought a huge number of death tolls. “The simplest” and “the cheapest” are required for the seismic retrofit schemes to upgrade those buildings, and this method is supposed to be “the cheapest” method depending on the selection of the kind of fibers. It will contribute to the earthquake disaster mitigation.

PROPOSED CONSTRUCTION METHOD

Drilling

The small holes are drilled at every grid intersection on the wall as shown in Fig.3.

Installation of FRP bands

FRP bands are installed on every diagonal two-holes as shown in Fig.4. If the FRP band is installed crossing a crack as shown in Fig.5, FRP can take full tension force because of the shape of a band, and the tension force transfers to the next FRP band through the un-cracked part of concrete. The advantages of this idea are:

- (1) The concrete wall does not need to have smooth surface.
- (2) There is no need to give epoxy-primer on the concrete wall surface.
- (3) The complete anchorage is secured for FRP bands to take full tension force.
- (4) It might be possible to reduce the amount of FRP material to obtain the necessary capacity gain.
- (5) It is possible to apply this method to the rehabilitation of the infill-brick wall.

A bundle of aramid fiber-strands were adopted as FRP bands so that it might sew the holes because of the following three reasons.

- (1) Strands are cheaper than the fabricated products. If the strips of FRP sheet are used, it costs much to produce the FRP sheet before installation. Strands directly come from the fiber-producing factory.
- (2) Aramid fiber is stronger when it touches the sharp edge.
- (3) In order to make a band, the overlap splicing is needed on every band, and a lot of work is needed. To reduce the work, the holes were sewed with a bundle of aramid fiber strands.

One sewing path is illustrated in Fig.6. A bundle of strands with resin sew holes in the zigzag path. The advantage of this path is that a bundle of strands do not cross in a hole, but the sewing path is split by the vertical lines. This was discussed in the pilot test.

Another sewing path is shown in Fig.7. A bundle of strands with or without epoxy resin sew holes in the diagonal directions. The advantage of this path is that a bundle of strands continues in the diagonal directions, and is expected to work as tension braces. It is somewhat difficult to pass a number of FRP bands in one hole. However this will be resolved by braiding the strands before installation.

PILOT TEST

Test specimens

Two scaled specimens were produced. One (W03N) was tested without strengthening. The other one (W02R) was strengthened with FRP bands before loading. The crushed part of the control specimen, W03N, was removed and repaired with new mortar, and the cracks were filled with epoxy resin. Then the wall panel was strengthened with this

1272 Kobayashi

proposed method (W03N-R). Three test specimens are listed in Table 1. The dimensions of a specimen and the reinforcing arrangement are shown in Fig.8. Each column has 10-D6 longitudinal bars. The wall panel has the round bars of 3mm in diameter at the interval of 100mm both horizontally and vertically.

The mechanical properties of the material are shown in Table 2. The lightweight concrete was used in order to obtain a low tensile strength and a low Young's modulus that are equivalent to those of normal low strength concrete. Aramid fiber strands were used considering the high strength when they contact the sharp edge.

RRP shear reinforcement ratio was defined as follow.

$$P_{wf} = \frac{a_f}{l_d \cdot t}$$

a_f : Sectional area of strands

l_d : Diagonal length of a grid

t : Thickness of wall panel

The effective strength of aramid strand was assumed to be 70% of tensile strength. The amount of FRP shear reinforcement was determined so that the shear capacity would increase by 30% using a shear capacity evaluation formula^[3] where the contribution of FRP was simply added to that of steel shear reinforcement.

Loading setup

Two oil jacks were set up on both side of specimen at the height of 425mm from the footing beam as shown in Fig.9. To introduce more shear force before reaching flexural capacity, the oil jacks were set up at as lower point as possible. The horizontal load was alternatively given by pushing the end of the beam.

Test results

Strengthening effect for the existing RC shear wall—Figure 10 shows the relation between the horizontal force and the horizontal displacement of W03N. It failed in shear mode at -200kN of shear force. The flexural capacity is 220kN in calculation. When the shear force reached -200kN, a critical shear crack was generated on the wall panel, and the specimen suddenly lost the bearing force. The shear cracks were induced on column top and bottom too.

W02R failed in shear mode at -240kN. Comparing with W03N, the shear capacity increased by 20%. 240kN is over the calculated flexural capacity, and the shear capacity would increase more, if it were not affected by bending yield. The horizontal load was concentrically given close to the column top, and the shear cracks were generated on the column tops. As a result of the shear deformation of the column tops, the top corner of wall panel was intensively pushed to one direction. Then the wall panel partially crushed, and the bearing force decreased gradually. However, the crushed part was well confined

by the aramid sewing bands, and the shear crack did not open and the crushed concrete didn't peel off. The horizontal load vs. displacement curves showed a stable behavior as shown in Fig.11, though the bearing force decreased.

In this pilot test only the wall panel was reinforced. However, the columns are to be reinforced in actual construction, and there might be more capacity gain if the horizontal load distributes on the top of wall panel.

Repairing and strengthening effect for the damaged RC shear wall--The holes were drilled on the grid intersection on the wall panel of W03N after loading test. Next, the wall panel was kept horizontal, and the epoxy resin was put on the panel and it sank in the cracks. After that, the sewing bands with epoxy resin were installed with the diagonal sewing path shown in Fig.7.

The column tops and bottom were wrapped with CF sheet without repairing the cracks. But the closed wrapping was not achieved because of the wall. The capacity and the rigidity completely recovered in both positive and negative loading directions. The capacity didn't increase. However the failure mode changed from that of W03N. The shear cracks on the column tops expanded, though the column tops were reinforced with CF sheet. Maybe this is due to no-injection of epoxy resin into the shear crack on the columns and no-closed wrapping of CF sheet. The column top deformed with shear force, and the crack developed along the interface between the wall panel top and the upper beam bottom. The shear crack at column bottom didn't expand. In the same way as that in W02R, the top corner of wall panel was intensively pushed to one direction. However the wall panel did not crush, and the slip failure occurred at the interface between the wall panel top and the upper beam bottom. The bearing force decreased gradually because the slip failure gradually progressed. The increase of the shear capacity may also depend on the strengthening method of columns, and the way to give horizontal force in the loading test.

Comparison of W02R and W03N-R--The shear crack occurred on the wall panel, and the wall panel partially crushed in W02R. The interface between the upper beam bottom and the wall panel top was sheared off, and the wall panel almost did not crush in W03N-R. In both specimens, the strengthening effect of sewing bands was recognized. If the sewing bands are installed after damage, the columns become relatively weaker than the wall panel. This will cause the shear off failure at the interface between the beam and the wall panel. This result means that the columns must be repaired and strengthened as well as the wall panel. Anyhow, it was proved that both the shear capacity and the deformability of the existing RC wall were improved by the proposed method.

TEST PROGRAM TO EVALUATE THE STRENGTHENING EFFECT

Outline of test program

To evaluate the strengthening effect, four new specimens were produced. The

1274 Kobayashi

dimensions of wall panel and columns are same as those of the pilot test specimens shown in Fig.8. To increase the flexural capacity, four longitudinal bars of D6 were added at the center of each column. To obtain the low strength normal concrete with high viscosity, one third of cement was replaced by the stone powder in the concrete mixing, and successfully the concrete with 26N/mm^2 in compressive strength and with 8cm of slump was obtained. To distribute the horizontal force on the top of wall panel, the dimension of the upper beam was increased to 190mm in width and 150mm in depth. The steel reinforcement in the wall panel and the steel shear reinforcement of the columns were same as those of the pilot test specimens.

The parameter of the test specimens is the number of aramid strands in a sewing band. No.1 is the control specimen without the sewing bands. No.2 to No.4 have 3, 6, 12 aramid strands in a sewing band. The diagonal sewing path shown in Fig.7 was adopted. The end of strands was winded around the columns in order to ensure the anchorage of sewing bands and to increase the shear capacity of columns. Under the upper beam and on the footing beam, the end of sewing band was not anchored into the beams, and the bundle of strands was spliced on the wall panel to make the completely closed bands.

The loading setup is same as that show in Fig.9, and the horizontal load was alternatively given at the center of the upper beam that is 475mm high from the top surface of the footing beam.

The mechanical properties of steel bars are same as those in the pilot test shown in Table 2. The characteristics of concrete used for new four specimens are summarized in Table 3.

Test results

The relations between the horizontal load and the horizontal displacement are shown in Fig.13. The control specimen (No.1) failed in shear mode. The critical shear cracks occurred and the mid-center of the wall panel crushed. The shear cracks occurred on columns, but they did not determine the shear capacity. No.1 reached the maximum load at the horizontal displacement of 2.6mm and quickly lost the bearing force. Figure14 shows the cracking pattern after loading test.

No.2 with a sewing band made of three strands got some shear capacity gain and didn't fail in the loading cycle where No.1 failed. After reaching the maximum load at the horizontal displacement of 3.5mm, the crush of wall panel was observed in very limited unit areas surrounded by the sewing bands. The applied load gradually decreased and the loading was stopped when it decreased to a half of the maximum load. No.3 and No.4 showed same behavior as that of No.2, and the maximum load and the deformation capacity increased according to the number of strands in a sewing band. The failure pattern of No.4 is shown in Fig.15. The test results are summarized in Table 4. Figure 16 shows the relation between the shear capacity gain percentage to the control specimen and the number of strands in a sewing band.

The shear capacity increased almost in proportion to the amount of fibers in a sewing

band, but it may have a limit because the crush of the wall panel will govern the capacity when the amount of fibers in a sewing band increases. Figure 17 shows the deformation capacity gain vs. the amount of fibers in a sewing band. The deformation capacity was defined as a displacement where the applied load decreased by 15% from the maximum load. It also increased almost in proportion to the amount of fibers in a sewing band, but it must have a limit because of the same reason for the shear capacity gain.

The strain gages were installed on the sewing band on each grid. Figure 18 shows the strain distribution of No.3 at the maximum load. The strain gages in the diagonal region of the wall panel showed a large value over 10000×10^{-6} . Figure 19 shows one example of the strain history to the loading cycles on a sewing band that is marked in Fig.18. When reaching the maximum load, the strain increased quickly, and immediately after the maximum load the strain increased more. It corresponds to the failure mode that the crush of wall panel occurred in the areas surrounded by sewing bands and the sewing bands were well resisting to swelling of the crushed concrete.

Strengthening effect of sewing bands

The wall panel is assumed to deform into a parallelogram as shown in Fig.20. The strain in the diagonal direction is

$$\varepsilon_f = \gamma \cdot \cos \theta \cdot \sin \theta$$

γ : Shear deformation angle

θ : Angle of the diagonal of the wall panel to the horizontal line

The horizontal load reached the maximum at about $\delta = 3mm$ in horizontal displacement in every specimen. Then ε_f is figured out to be 0.003. If the sewing bands work as the tension braces, their contribution to the shear capacity gain is

$$\Delta V_{TB} = \varepsilon_f \cdot E_f \cdot a_f \cdot n_{TB} \cdot \cos \theta$$

n_{TB} : The number of strands in a diagonal direction that contribute to the shear capacity gain

a_f : Sectional area of a strand

E_f : Young's modulus of the fiber

ΔV_{TB} is figured out to be 3.52kN, 7.05kN and 14.1kN for No.2, No.3 and No.4 respectively. They are, however, too small in comparison with the test results shown in Table 4. The value of 0.003 for ε_f is also too small in comparison with the measured strain on the sewing band. This means that the shear capacity gain is obtained by another mechanism as well as the tension bracing effect of the sewing bands. And the strain of the sewing bands will be also caused by another mechanism.

The horizontal force can transfer through the strut as shown in Fig.21. If the strut has the dimension shown in Fig.21, the contribution of the strut to the shear capacity gain is

$$\Delta V_{CB} = (h + D) \cdot t \cdot \Delta \sigma_{CB} \cdot \cos^2 \varphi$$

1276 Kobayashi

t : Thickness of wall panel

h : Height of wall panel

D : Overall depth of column

$\Delta\sigma_{CB}$: Compressive strength gain of the strut due to the confining effect by the sewing bands

If the compressive strength of the strut is assumed to increase due to the confining effect of the sewing bands, it contributes to the horizontal load capacity gain. The compressive strength gain of the strut is figured out to be 1.72N/mm², 1.87N/mm² and 4.64N/mm² for No.2, No.3 and No.4 respectively from $\Delta V_{exp}-\Delta V_{TB\ cal}$ in Table 5. Those values look too large, but it would be a possible strength gain of confined concrete. More test data will be needed.

Amount of sewing bands

To evaluate the confining effect, the volume fraction of fibers in sewing bands to the wall panel is more reasonable than the area fraction. Here the fiber volume fraction to one grid of concrete wall panel is defined as follow, considering the ratio of young's modulus of fiber materials to that of concrete.

$$\rho_f = \frac{4(l_d + t) \cdot A_f}{l \cdot h \cdot t} \cdot \frac{E_f}{E_c}$$

l_g : Horizontal length of a grid

h_g : Height of a grid

l_d : Diagonal length of a grid ($=\sqrt{l_g^2 + h_g^2}$)

A_f : Sectional area of a bundle of strands

E_f : Young's modulus of fiber

E_c : Young's modulus of concrete

The relation between $\Delta\sigma_{CB\ exp}$ and ρ_f (%) for the test results is obtained by the regression analysis as follow.

$$\Delta\sigma_{CB\ exp} = 1.53\sqrt{\rho_f}$$

If the dimension of concrete wall panel is 4800(l) \times 2400(h) \times 120(t) mm and it is divided into 9 \times 9 grids, the required volume of aramid strands is figured out from the above equations to be 1.476 \times 10⁷ mm³. The specific gravity of aramid strand is 0.00139g/mm³. Then, 20.4 \times 10³ g of aramid strand would be required to strengthen the wall and 700kN of the shear capacity gain is obtained. On the other hand, if this concrete wall is strengthened by CF sheet according to the SR-CF system^[4], three layers of CF sheet with 300g/m² in each direction is required. The weight is 40 \times 10³ g. The ratio of the required weight of aramid strand to CF sheet is about 0.5, and in addition the cost of strand is much less than the fabricated product such as CF sheet. If it is assumed that the cost of strand is one-fifth of fiber sheet, the cost of sewing system is possibly reduced to less than one-tenth of fiber sheet wrapping system depending on the kind of fibers.

CONCLUSIONS

The proposed method was proved to be effective both mechanically and economically. The sewing bands will work as the confining reinforcement to the wall panel as well as the tension braces. The shear capacity and the deformability increased in proportion to the number of strands in a sewing band. There is a possibility to be able to reduce the amount of fibers in the sewing system in comparison with fiber sheet wrapping system in order to obtain the same shear capacity gain and the deformation capacity gain. This strengthening method is possibly applicable to the infill-brick wall to keep the bricks inside the frame and to expect them to carry the horizontal force. Also this method is expected to work to avoid the collapse of the infill-brick wall to out of frame even when it receives the seismic force in the orthogonal direction.

ACKNOWLEDGMENT

This study is financially supported by the Grants-in-Aid for Scientific Research (C)(2) No. 16560493, JSPS. The author would like to express his great appreciation to them.

REFERENCES

- 1 Architectural Institute of Japan, Japan Society of Civil Engineers and The Japanese Geotechnical Society, "Report on the Damage Investigation of the 1999 Kocaeli Earthquake in Turkey", (1991).
- 2 Binici, B. and Bayrak, O., "Punching Shear Strengthening of Reinforced Concrete Flat Plates Using Carbon Fiber Reinforced Polymers", Journal of Structural Engineering, ASCE, Vol.129, No.9, pp.1173-1182.
- 3 Architectural Institute of Japan, "Ultimate Strength and Deformation Capacity of Buildings in Seismic Design", (1990).
- 4 Katsumi Kobayashi, Toshiyuki Kanakubo and Yasuo Jinno, "Seismic Retrofit of Structures using Carbon Fibers", VIII Mexican Symposium on Earthquake Engineering, Tlaxcala, Mexico, September 2004.

Table 1--Pilot test specimens

Specimen	Number of strands	Remarks
W03N	0	Control specimen
W02R	10	Strengthening effect for existing wall. Compare with W03N (No.3).
W03N-R	10	Strengthening effect after damage. Compare with W03N (No.3).

Table 2--Mechanical properties of materials

Concrete (N/mm ²)			
Specimen	Compressive strength	Tensile strength	Young's modulus
W03N	36.8	2.35	—
W02R	40.2	2.59	1.74×10^4
Steel (N/mm ²)			
Re-bars	Yield strength	Tensile strength	Young's modulus
D6	353	544	1.86×10^5
ϕ 4	276	389	1.94×10^5
ϕ 3	283	435	1.96×10^5
Aramid strand (N/mm ²)			
Diameter of filament	Density	Tensile strength	Young's modulus
12 μ m	6000dn	3430	7.25×10^4

Table 3--Characteristics of concrete

Concrete (N/mm ²)			
Specimen	Compressive strength	Tensile strength	Young's modulus
No.1-No.4	26	1.9	2.14×10^4

Table 4--Test results

Specimen	Number of strand	Maximum load (kN)	Capacity gain (kN)	Deformation capacity* (mm)
No.1	0	193.0	-	2.9
No.2	3	209.4	16.4	4.2
No.3	6	213.5	20.5	4.6
No.4	12	240.2	47.2	5.3

* It is defined as the horizontal displacement where the bearing force decreased by 15% from the maximum

Table 5--Strengthening effect of sewing bands

	ΔV_{exp} (kN)	n_{TB}	$\Delta V_{TB cal}(\text{kN})$ $\varepsilon_f=0.003$	$\Delta V_{exp}-\Delta V_{TB cal}$ (kN)	$\Delta \sigma_{CB cal}$ (N/mm ²)	ρ_f (%)	$\Delta V_{CB cal}$ (kN)	ΔV_{cal} (kN)
No.2	16.4	36	3.52	12.9	1.72	1.47	14.5	18.1
No.3	21.1	72	7.05	14.0	1.87	2.94	20.6	27.6
No.4	48.9	144	14.1	34.8	4.64	5.88	29.1	43.2



Fig.1—Collapse of the infill-bricks out of the frame



Fig.2—Collapse of the building in the shape of pancake

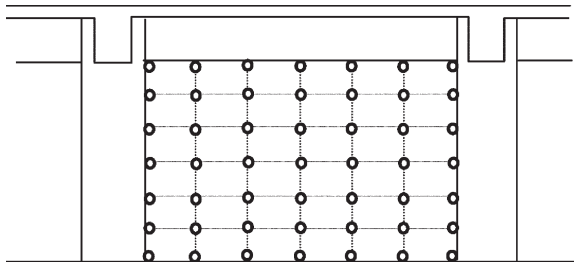


Fig.3—Drilling on the wall panel

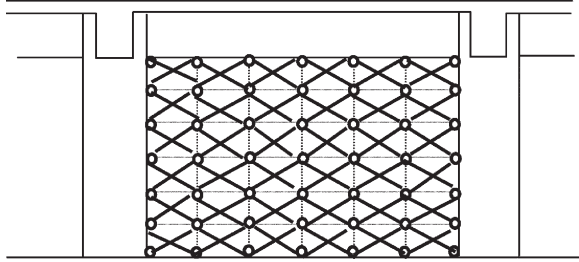


Fig. 4—Installation of FRP bands

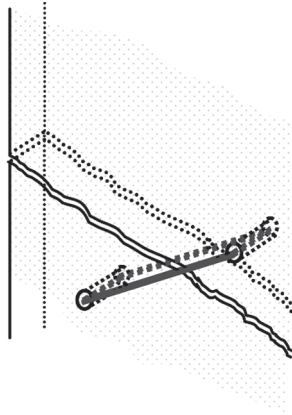


Fig.5—A FRP band over the crack

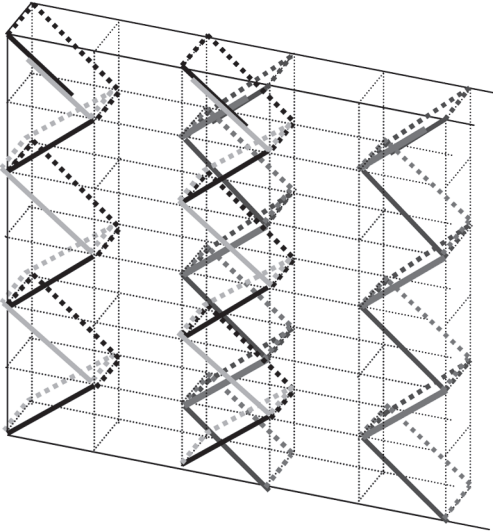


Fig.6—A zigzag sewing path

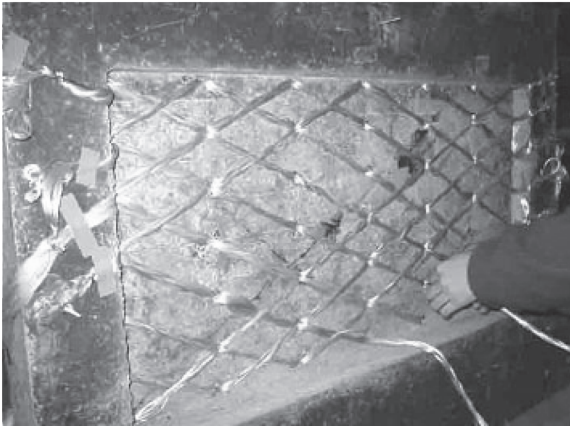
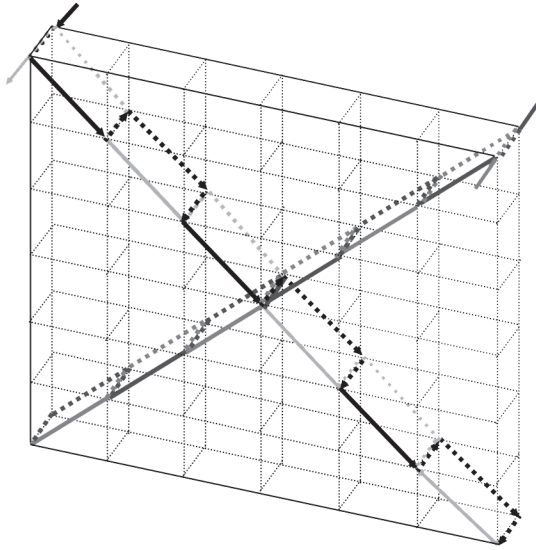


Fig. 7—Diagonal sewing path

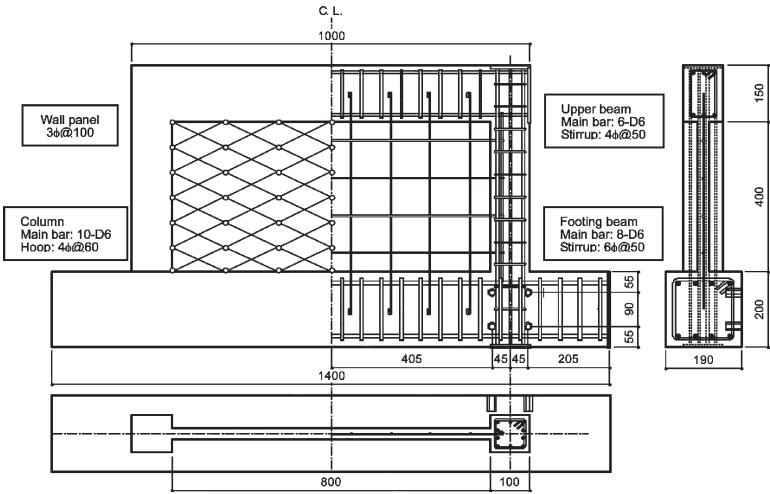


Fig. 8—Dimensions and reinforcing arrangement of the test specimen

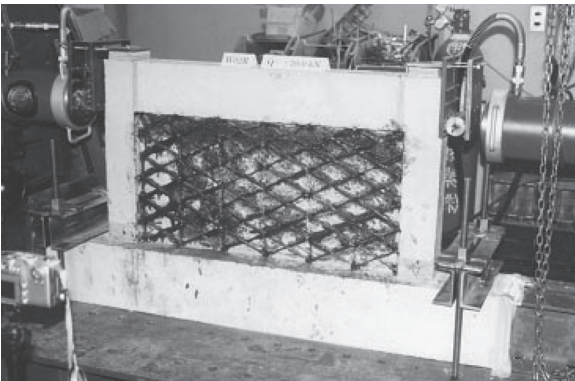


Fig. 9—Loading setup

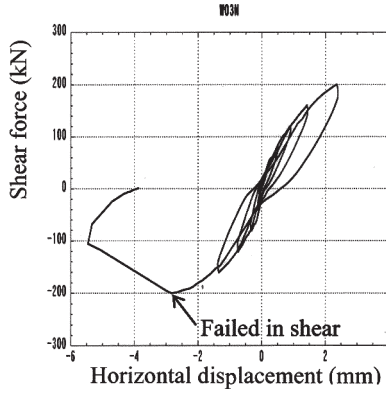


Fig.10—Applied load-horizontal displacement relation (W03N)

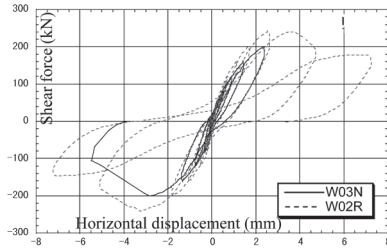


Fig.11—Applied load-horizontal displacement relation (W02R)

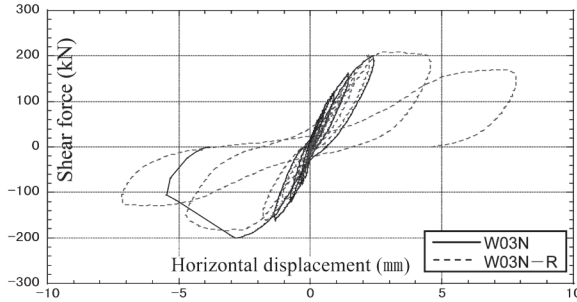


Fig.12—Applied load-horizontal displacement relation (W03N-R)

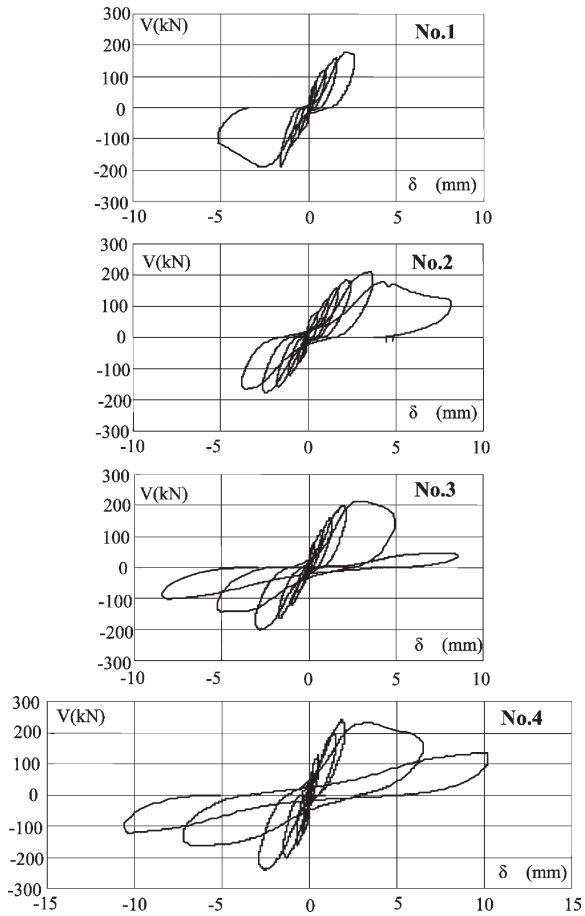


Fig. 13—Horizontal load – displacement relations

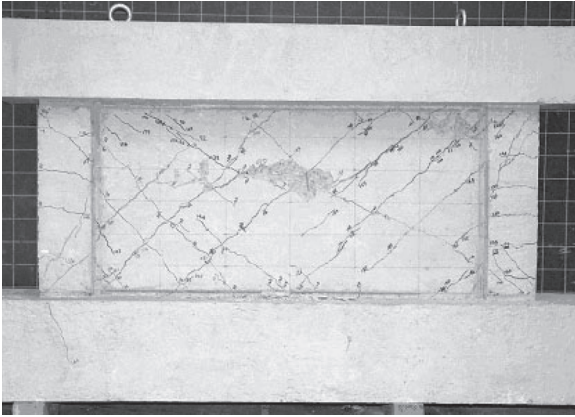


Fig. 14—Cracking pattern of No.1 specimen



Fig. 15—Ultimate failure mode of No. 4 specimen

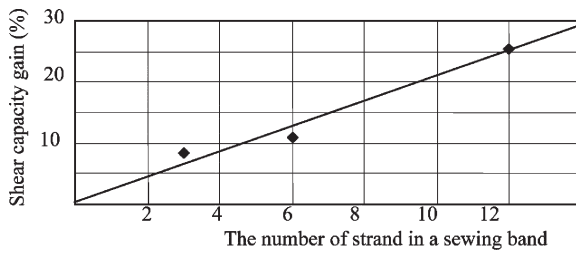


Fig. 16—Shear capacity gain

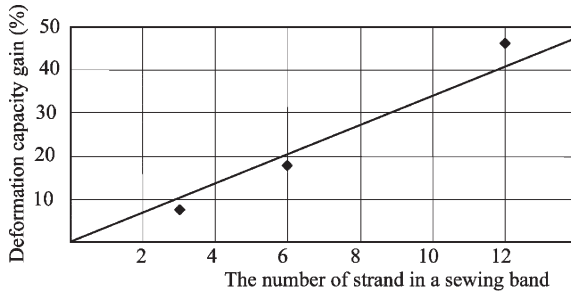


Fig. 17—Deformation capacity gain

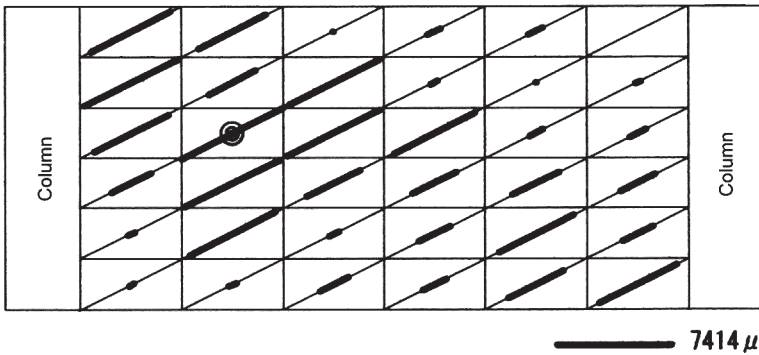


Fig. 18—Strain distribution on the sewing bands of No.3 specimen

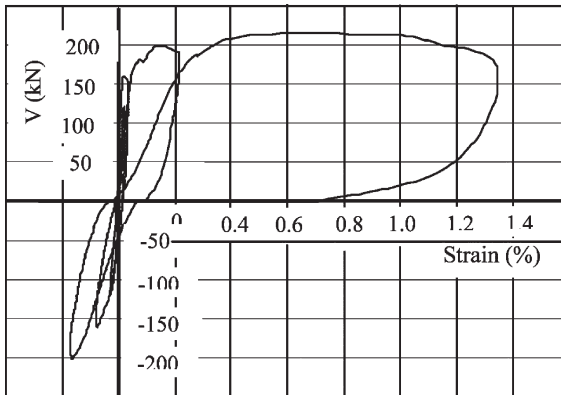


Fig. 19—A strain history to the loading cycles

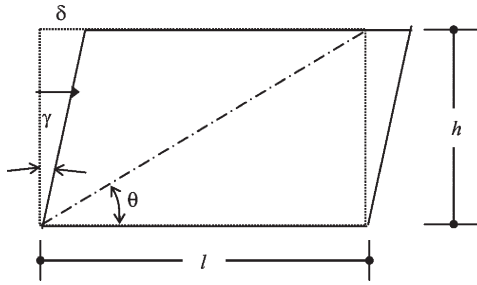


Fig. 20—Assumed deformation of the wall panel

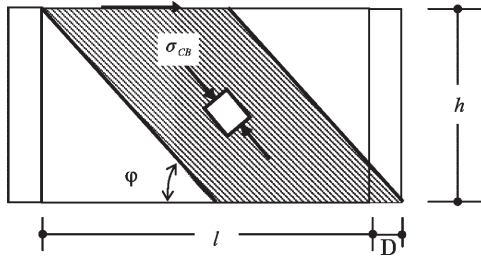


Fig. 21—Truss action on the wall panel